ARTICLES

Magnetothermal conductivity of $La_{0.8}Ca_{0.2}MnO_3$

Baoxing Chen, A. G. Rojo, and C. Uher
Department of Physics, University of Michigan, Ann Arbor, Michigan 48109

H. L. Ju* and R. L. Greene
Center for Superconductivity Research, Department of Physics, University of Maryland, College Park, Maryland 20742
(Received 27 January 1997)

We have studied thermal conductivity, thermopower, and resistivity of bulk polycrystalline $La_{0.8}Ca_{0.2}MnO_3$. Large changes in the magnetothermal conductivity of about 15% and the thermopower as large as 80% were found in addition to a large magnetoresistivity of 80% around the magnetic transition temperature at 240 K. The temperature dependence of the thermal conductivity displays a striking dip, while the resistivity and the thermopower have a peak near 240 K. The temperature and field dependences of the thermal conductivity are attributed to the scattering of the phonons by spin fluctuations. [S0163-1829(97)05024-8]

The discovery of colossal magnetoresistance (CMR) in the perovskite-based $La_{1-x}A_xMnO_3$ compounds[1,2] (A =Ca,Sr,Ba) has led to several reports on the interplay between their fascinating transport properties and the underlying magnetic structure.[3–5] While much progress has been made on both the experimental and theoretical fronts, the mechanism of CMR is still not fully understood. The double-exchange model of Zener[6] can qualitatively explain the simultaneous appearance of metallic conduction and ferromagnetism, but it cannot adequately capture several aspects of the resistivity data. Consequently, an extension of coupling to lattice degrees of freedom in the form of the Jahn-Teller (JT) effect has been considered essential in understanding the physics of CMR.[7] Among various aspects of transport studies in these materials, thermopower has attracted much attention recently[4,9] because it is a parameter sensitive to the nature of the carriers and their interaction with spins. Different carrier signs are predicted depending on the degree of JT distortion.[10] Thus, in the absence of the static JT distortion, the carriers are predicted to be electrons. On the other hand, with a sufficiently large static JT distortion the carriers take on a holelike character. This may have been the reason for different thermopower signs in the two reports published recently. In their work on thick films of $La_{0.67}Ca_{0.33}MnO_3$ prepared by metallorganic decomposition process, Chen *et al.*[4] reported negative and rising thermopower with increasing temperature but no peak near T_c. In contrast, Jaime *et al.*[8] measured positive thermopower that displayed a clear peak near T_c in their laser-ablated films of similar composition.

To better understand the nature of electron-phonon coupling and the JT distortion in these materials we made measurements of the thermal conductivity along with the studies of the electrical resistivity and thermopower on bulk, sintered samples with $x=0.2$. We found that the thermopower in these samples is positive and displays a peak around T_c in accord with the theoretical predictions of Ref. 10. We also found a large difference between the activation energies governing the temperature dependence of the thermopower and the electrical resistivity above T_c, which points to the polaronic character of the charge carriers in this temperature domain. The strong coupling between the lattice and spins is manifested by a dip in the temperature dependence of the thermal conductivity at T_c and its disappearance when a magnetic field is applied to the sample.

The samples were prepared by mixing stoichiometric quantities of La_2O_3, $CaCO_3$, and $MnCO_3$ that were repeatedly grinded and fired at 1200 °C until a single phase was obtained. During the final stage the powder was pelletized and annealed at 1300 °C in air for 24 h to make a dense sample. For measurements of the thermopower and thermal conductivity we used the steady-state method. A thermal gradient was generated by a resistive heater mounted at one end of the sample and was measured by using a chromel-constantan thermocouple. The temperature range from 2 to 300 K was covered by a cryostat equipped with a superconducting magnet generating fields up to 6 T. The magnetization and the resistivity data were collected using a Quantum Design superconducting quantum interference device magnetometer.

Figure 1 shows the temperature dependence of zero-field resistivity, resistivity measured in the field of 5 T, and the magnetoresistivity defined as $\Delta\rho/\rho(0)=[\rho(0)-\rho(5\ \mathrm{T})]/\rho(0)$. At low temperatures the sample is magnetically ordered and the resistivity has a metallic character with a value of 6 mΩ cm, a rather high resistivity symptomatic of the sintered nature of the sample. As the temperature increases and the magnetic transition is approached near $T_c=240$ K (see the inset in Fig. 1), the resistivity rises sharply and reflects the influence of the increasing magnetic disorder in conjunction with the formation of magnetic polarons, possibly modified by the Jahn-Teller effect. An external magnetic field has a tendency to align the ionic spins and destroy the polaron

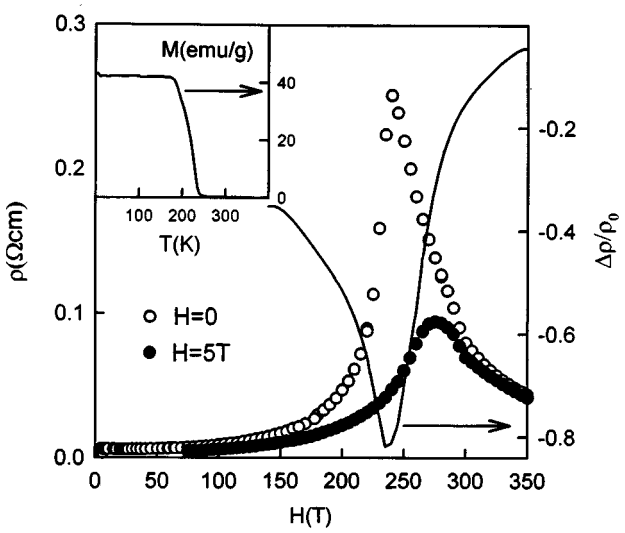

FIG. 1. Temperature dependences of zero-field resistivity $\rho(0)$, resistivity measured at 5 T, and magnetoresistance $\Delta\rho/\rho(0)$ at 5 T. The inset shows the temperature dependence of magnetization at $H=0.05$ T.

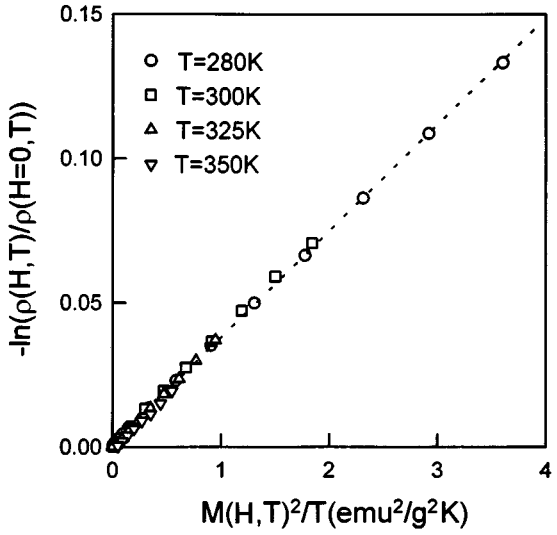

FIG. 3. Plot of $\ln[\rho(H,T)/\rho(H=0,T)]$ vs $M^2(H,T)/T$ at 280, 300, 325, and 350 K. The field ranges from 0 to 5 T.

state. In particular, the electron bandwidth becomes larger as the angle between the spins decreases. As a consequence, the resistivity measured in the magnetic field is much reduced and the magnetoresistivity reaches very large negative values, which is referred to as the CMR effect. The field has its greatest influence near T_c; however, substantial magnetoresistance in our samples persists down to below 50 K. The intimate relation between the transport behavior and the magnetic state of the material is seen clearly from the data in Fig. 2, where $\rho(H,T)$ is plotted against the magnetization $M(H,T)$. Similar plots have been reported previously by Hundley *et al.*[3] for their pulsed-laser deposited films of $La_{0.7}Ca_{0.3}MnO_3$ and by us for thick films of $La_{0.66}Ca_{0.33}MnO_3$. It is clear, referring to Fig. 2, that the correlation between $\rho(H,T)$ and $M(H,T)$ is strong from about 200 K up to T_c, but it breaks down for temperatures below 200 K. Above the magnetic phase transition, the nature of transport changes dramatically and the resistivity acquires a distinctly semiconducting (activated) character. Assuming a simple exponential dependence of the form $\rho=\rho_0\exp(E_\rho/k_BT)$, a fit to the data of Fig. 1 above T_c yields $\rho_0=881$ $\mu\Omega$ cm and an activation energy of $E_\rho=122$ meV. The latter is in good agreement with the values reported previously[3,8,11] even though the form of the samples and the doping levels are quite different. The resistivity continues to be correlated with the magnetization even well above T_c, but the functional dependence is now different, $\rho(H,T)=\rho(T)\exp[-M^2(H,T)/k_BT]$, as seen in Fig. 3.

The results of the thermopower measurements are shown in Fig. 4. The thermopower is positive throughout the temperature range investigated, suggesting that the charge carriers are holes and, according to Ref. 10, signaling the pres-

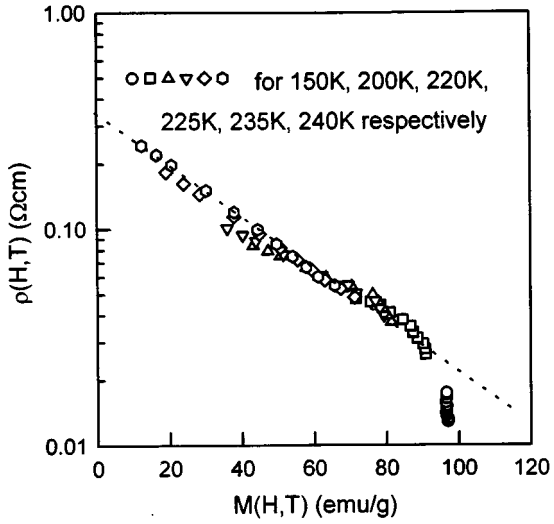

FIG. 2. Magnetoresistance $\rho(H,T)$ on a logarithmic scale vs magnetization at different temperatures.

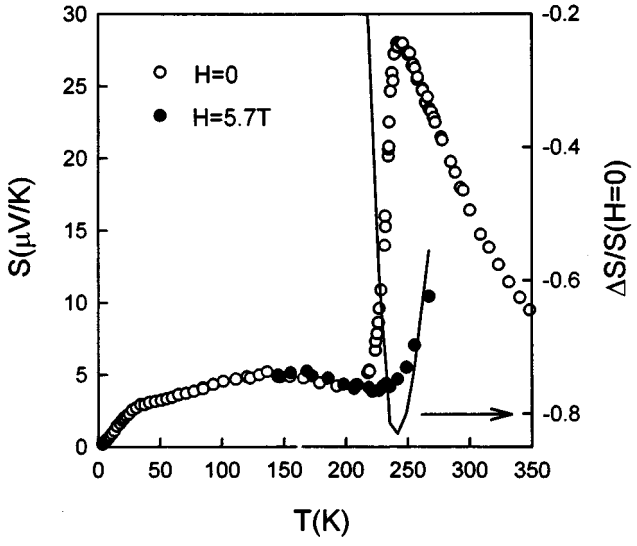

FIG. 4. Temperature dependence of zero-field thermopower $S(0)$, thermopower measured in the field of 5.7 T, and magnetothermopower $\Delta S/S(0)$.

ence of a strong static JT distortion. A large peak (28 μV/K) is seen near 240 K, reminiscent of the peak in the resistivity. Earlier measurements[12] on nominally the same compounds indicated about twice the value of the peak thermopower; however, the magnetic transition in this case was at a considerably lower temperature of 208 K. There are two additional peaks or breaks on the thermopower curve of Fig. 4 below T_c: one around 30 K and the other one near 150 K. We do not have concrete evidence for any specific physical mechanism that might be at play, but speculate that the anomaly near 30 K might be a signature of the phonon-drag effect, while the peak near 150 K could be associated with scattering by magnetic impurities or magnons.[13] Resolution of these issues awaits measurements on single crystals where the influence of impurities (both magnetic and nonmagnetic) can be better controlled than in the case of sintered samples.

High-temperature thermopower (the data above the peak) fits very well the functional form $S=k_B/e[E_s/k_BT+B]$ with the gap $E_s=16.3$ meV and $k_BB/e=-37.6$ μV/K. Two things are interesting about the value of the gap E_s. First, the gap obtained from the thermopower measurements is nearly an order of magnitude smaller than the activation gap governing the electrical resistivity E_ρ. As originally pointed out by Mott and Davis[14] and further discussed in Ref. 8, the reason for this discrepancy is the thermal activation nature of the hopping transport at high temperatures. The carrier mobility and therefore electrical conductivity contain an exponential term $\exp[-(\varepsilon_F+W_H)/k_BT]$, where W_H is the hopping energy, while from the perspective of the thermopower the hops take place between energetically equivalent sites and a reference point for the entropy carried by the carriers is the Fermi level. This leads to the thermopower formula mentioned previously, which does not contain an exponential energy term. The difference between the experimentally determined activation energies for the resistivity and thermopower is then $E_\rho-E_s=\varepsilon_F+W_H-\varepsilon_F=W_H\cong 106$ meV. A large difference between E_ρ and E_s is a strong indication of the polaron transport with the polaron energy given by twice the value of the hopping energy, i.e., about 212 meV. The second interesting point concerns virtually the same magnitude of the gap energy E_s observed in Ref. 8 and in the present work. This is in spite of the facts that the samples are structurally very different, are doped with different amounts of calcium, and are subjected to very different annealing cycles. If one assumes that the polaron energy relates to the size of the polaron, one arrives at the conclusion that the polaron size does not seem to be sensitive to the preparation conditions and the doping level of the material.

Measurements of the thermal conductivity represent an attempt to study heat transport in the CMR compounds. Figure 5 shows the temperature dependence of thermal conductivity obtained in zero magnetic field $\kappa(0)$, thermal conductivity $\kappa(5.7\ \mathrm{T})$ measured in the field of 5.7 T, and the quantity $\Delta\kappa/\kappa\equiv[\kappa(5.7\ \mathrm{T})-\kappa(0)]/\kappa(0)$. The general shape of $\kappa(0)$ is that of a polycrystalline dielectric solid. Indeed, making use of the electrical resistivity data and applying the Wiedemann-Franz law, we estimate the electronic part of the thermal conductivity to be at most 1% of the total thermal conductivity in the entire temperature range investigated. The dominant feature of $\kappa(0)$ at low temperatures is the dielectric peak near 35 K. At temperatures below this peak the thermal conductivity decreases rapidly and near 4 K it approaches a T^2 variation with temperature. Whether the ultimate T^3 dependence characteristic of phonon boundary scattering would be reached could only be answered by extending the measurements below 1 K. On the high-temperature side of the peak the conductivity decreases, presumably as a result of phonon-phonon umklapp scattering. There is a notable break on the curve near 150 K that marks a more rapid decrease in $\kappa(0)$ and leads to a rather sharp minimum near 240 K. Although a small part of the rise above 240 K is due to an unavoidable radiation heat loss that we estimate as about 7% at 300 K, there is no doubt that the thermal conductivity displays a clear identifying characteristic of the influence of spins on the heat transport. In this case

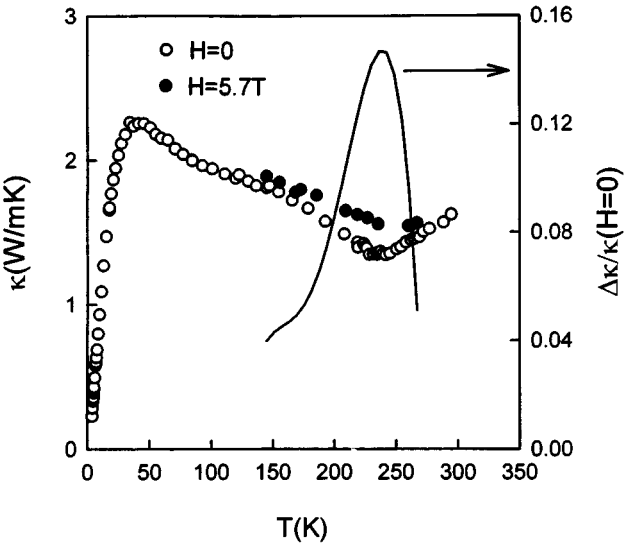

FIG. 5. Temperature dependence of thermal conductivity $\kappa(0)$, thermal conductivity measured at 5.7 T, and magnetothermal conductivity $\Delta\kappa/\kappa(0)$.

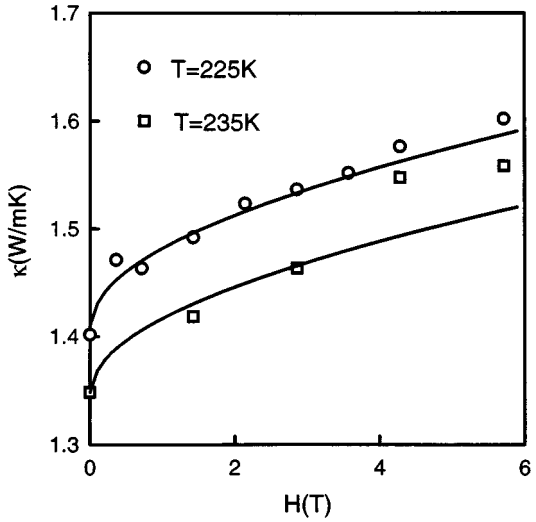

FIG. 6. Plot of thermal conductivity $\kappa(H)$ vs applied magnetic field at 225 and 235 K. The solid curves are fits to the experimental data using δM based on Eq. (1). The following values were used for both temperatures: $J=0.02$ eV, $a=8$ Å, and $l_{\mathrm{mag}}(H=0)/l_{\mathrm{nonmag}}=\frac{1}{2}$.

it is not as much the self-localization nature of the polarons that impedes the energy flow associated with the charge carriers (it certainly does so, but the carrier contribution to the heat flow is only a minute fraction of the total heat flow) but rather it is the spin fluctuations that impedes the heat flow of phonons. Measurements of the thermal conductivity in a magnetic field make this point quite clear. The external magnetic field tends to suppress the spin fluctuations. The curve representing $\Delta\kappa/\kappa(0)$ clearly delineates the regime of strong phonon-spin fluctuations scattering.

Due to the presence of spin fluctuations, the phonon mean free path $l_{\rm ph}$ can be expressed as $1/l_{\rm ph}=1/l_{\rm nonmag}+1/l_{\rm mag}$, where $l_{\rm nonmag}$ represents the phonon mean free path limited by phonon-phonon, umklapp, phonon-impurity scattering, etc., and $l_{\rm mag}$ represents that limited by phonon-spin fluctuations scattering. The presence of strong phonon-spin coupling is evident in the recent study on the magnetovolume effect in La-Ca-Mn-O perovskites.[15] In our case, the phonons experience scattering proportional to the deviation of magnetization (δM) from its saturation value, i.e., $1/l_{\rm mag} \sim \delta M(T,H)$. For a ferromagnetic spin lattice, thermal fluctuations of the magnetization $\delta M(T,H)$ can be written as[16]

$$\delta M(T,H)=\int d^3k\{\exp[(Dk^2+\mu_B H)/k_B T]-1\}^{-1}, \tag{1}$$

where $D=2SJa^2$ and $k_{\rm max}\sim\pi/a$. Here J is the exchange integral, S is the total spin, and a is the lattice constant. At finite T, a higher H will cause a smaller δM, a larger $l_{\rm mag}$, a larger $l_{\rm ph}$, and thus a higher thermal conductivity. In Fig. 6 we show plots of the thermal conductivity as a function of magnetic field at 225 and 235 K. The solid curves show the fit to the experimental data using δM based on Eq. (1) and good agreement between the theory and experiment is obtained for both temperatures. Some deviations for the data at $T=235$ K, particularly for the points at higher fields, could be attributed to other contributions to δM in addition to the thermal fluctuations, e.g., the critical fluctuations of the magnetization. Referring to the temperature dependence, a peak in δM at the critical temperature will cause a minimum in the thermal conductivity just as we observe in our experiment. Similar dips in the thermal conductivity were observed previously in CoF_2 (Ref. 17) and MnO.[18]

In conclusion, we have studied thermal and electrical transport properties in bulk, sintered $La_{0.8}Ca_{0.2}MnO_3$ and found that the charge carriers have a holelike character and polarons play an essential role in the carrier dynamics. We have established that the carrier contribution to the heat flow is small and the spin fluctuations are effective in scattering the phonons. Transport studies on well characterized single crystals would be most desirable because the various subtle features of the transport would be magnified and easier to resolve.

The authors wish to acknowledge useful discussions with Dr. D. T. Morelli. This work was supported in part by ONR Grant No. N00014-92-J-1335.

*Present address: Lawrence Berkeley Laboratory, Bldg. 66-312, Berkeley, CA 94720.

[1] R. von Helmolt, J. Wecker, B. Holzapfel, L. Schultz, and K. Samwer, Phys. Rev. Lett. **71**, 2331 (1993).

[2] S. Jin, T. H. Tiefel, M. McCormack, R. A. Fastnacht, R. Ramesh, and L. H. Chen, Science **264**, 413 (1994).

[3] M. F. Hundley, M. Hawley, R. H. Heffner, Q. X. Jia, J. J. Neumeier, J. Tesmer, J. D. Thompson, and X. D. Wu, Appl. Phys. Lett. **67**, 860 (1995).

[4] Baoxing Chen, C. Uher, D. T. Morelli, J. V. Mantese, A. M. Mance, and A. L. Micheli, Phys. Rev. B **53**, 5094 (1996).

[5] H. L. Ju, C. Kwon, Qi Li, R. L. Greene, and T. Venkatesan, Appl. Phys. Lett. **65**, 2108 (1994).

[6] C. Zener, Phys. Rev. **82**, 403 (1951).

[7] A. J. Millis, P. B. Littlewood, and B. I. Shraiman, Phys. Rev. Lett. **74**, 5144 (1995).

[8] M. Jaime, M. B. Salamon, K. Pettit, M. Rubinstein, R. E. Treece, J. S. Horwitz, and D. B. Chrisey, Appl. Phys. Lett. **68**, 1576 (1996).

[9] M. Jaime, M. B. Salamon, M. Rubinstein, R. E. Treece, J. S. Horwitz, and D. B. Chrisey, Phys. Rev. B **54**, 11 914 (1996).

[10] Jun Zhang, A. R. Bishop, and H. Roder, Phys. Rev. B **53**, R8840 (1996).

[11] M. S. Rzchowski, J. O'Donnell, B. M. Hinaus, and M. Onellion (unpublished).

[12] J. Tanaka, M. Umehara, S. Tamura, M. Tsukioka, and S. Ehara, J. Phys. Soc. Jpn. **51**, 1236 (1981).

[13] I. Ya. Korenblit and Yu. P. Lazarenko, Zh. Eksp. Teor. Fiz. **60**, 1548 (1971) [Sov. Phys. JETP **33**, 837 (1971)].

[14] N. F. Mott and E. A. Davis, *Electronic Processes in Non-Crystalline Materials* (Oxford University Press, New York, 1979).

[15] M. R. Ibarra, P. A. Algarabel, C. Marquina, J. Blasco, and J. Garcia, Phys. Rev. Lett. **75**, 3541 (1995).

[16] C. Kittel, in *Quantum Theory of Solids* (Wiley, New York, 1963).

[17] G. A. Slack, Phys. Rev. **122**, 1451 (1961).

[18] G. A. Slack and R. Newman, Phys. Rev. Lett. **1**, 359 (1958).